Superconducting and antiferromagnetic properties of dual-phase V$_3$Ga

Michelle E. Jamer, Brandon Wilfong, Vasiliy D. Buchelnikov, Vladimir V. Sokolovskiy, Olga N. Miroshkina, Mikhail A. Zagrebin, Danil R. Baigutlin, Jared Naphy, Badih A. Assaf, Laura H. Lewis, Aki Pulkkinen, Bernardo Barbiellini, Arun Bansil, and Don Heiman

View Online   Export Citation   CrossMark

ARTICLES YOU MAY BE INTERESTED IN

Superconducting and antiferromagnetic properties of dual-phase V$_3$Ga

Michelle E. Jamer,[1,a]   Brandon Wilfong,[1]   Vasiliy D. Buchelnikov,[2,3]   Vladimir V. Sokolovskiy,[2,3]
Olga N. Miroshkina,[2,4]   Mikhail A. Zagrebin,[2,3,5]   Danil R. Baigutlin,[2,4]   Jared Naphy,[1]   Badih A. Assaf,[6]
Laura H. Lewis,[7]   Aki Pulkkinen,[4,8]   Bernardo Barbiellini,[4,9]   Arun Bansil,[9] and Don Heiman[9]

AFFILIATIONS

[1]Physics Department, United States Naval Academy, Annapolis, Maryland 20899, USA
[2]Faculty of Physics, Chelyabinsk State University, 454001 Chelyabinsk, Russia
[3]National University of Science and Technology "MISiS," 119049 Moscow, Russia
[4]Department of Physics, School of Engineering Science, LUT University, FI-53850 Lappeenranta, Finland
[5]National Research South Ural State University, 454080 Chelyabinsk, Russia
[6]Department of Physics, University of Notre Dame, Notre Dame, Indiana 46556, USA
[7]Chemical Engineering Department, Northeastern University, Boston, Massachusetts 02115, USA
[8]Département de Physique and Fribourg Center for Nanomaterials, Université de Fribourg, CH-1700 Fribourg, Switzerland
[9]Physics Department, Northeastern University, Boston, Massachusetts 02115, USA

[a]Author to whom correspondence should be addressed: jamer@usna.edu

ABSTRACT

The binary compound V$_3$Ga can exhibit two near-equilibrium phases, the A15 structure that is superconducting and the Heusler D0$_3$ structure that is semiconducting and antiferromagnetic. Density functional theory calculations show that these two phases are nearly degenerate, being separated in energy by only ± 10 meV/atom. Our magnetization measurements on bulk-grown samples show antiferromagnetism and superconducting behavior below 14 K. These results indicate the possibility of using V$_3$Ga for quantum technology devices exploiting the coexistence of superconductivity and antiferromagnetism in a dual-phase material.

https://doi.org/10.1063/5.0015535

Superconductivity and magnetism were once thought to be mutually exclusive because magnetic fields are efficient at closing the superconducting gap. Nevertheless, it was found that superconductivity has been found in 3d materials with magnetic transition-metal atoms and magnetic lattices as well.[1] High-T_c cuprate superconductors, for example, were found to have exceedingly strong magnetic exchange,[2] while Fe-based superconductors were found to have large Fe moments of several Bohr magnetons.[3,4] Also of interest here are the binary vanadium compounds, such as V$_3$Al, which belong to a class of simple superconductors with an A15 (β-W) crystal structure.[5–8] Interestingly, V$_3$Al has also been synthesized in a non-superconducting D0$_3$ Heusler phase with antiferromagnetic (AFM) order.[9] This D0$_3$ phase of V$_3$Al was predicted to be a gapless semiconductor[10,11] and found experimentally[9] to be a G-type antiferromagnet having a Néel temperature of $T_N = 600$ K. It is clear that V$_3$Z-type compounds represent a class of hybrid materials that could possess both superconducting and magnetic properties at the same temperature, which could provide potential

next-generation platforms for hosting Majorana modes[12] for applications in possible fault-tolerant quantum computer hosting and other quantum technology applications.

Another well-known binary compound in the vanadium family is V$_3$Ga, which has been used in superconducting applications for many years.[13] The remarkable low-temperature elastic, electric, magnetic, and superconducting properties of this material have been investigated extensively both experimentally and theoretically (see, e.g., Refs. 14–20). The critical temperature of superconducting V$_3$Ga in the A15 phase is 15 K.

V$_3$Ga can exist in two near-equilibrium phases, the A15 superconducting phase and the AFM D0$_3$ phase—an interesting and potentially useful result of their similar formation energies. Since the arrangement of atoms in binary V$_3$Ga can accommodate both D0$_3$ and A15 structures (Fig. 1), one must study the stability of these two phases using density functional theory (DFT). DFT was used here to compute the formation energies for various crystalline and magnetic
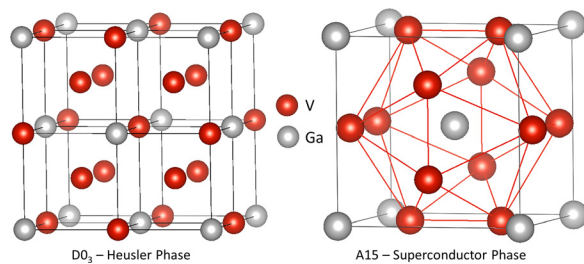
FIG. 1. $D0_3$ (space group: $Fm\bar{3}m$, no.: 225, and prototype, BiF_3) and β-W A15 (space group: Pm3n, no.: 223, and prototype, Cr_3Si) crystal structures of V_3Ga.

structures. Previous calculations for the $D0_3$ structure of V_3Ga by Galanakis *et al.*[11] predict a Heusler G-type AFM phase with a Néel temperature well above room temperature, which makes the compound attractive for spintronic applications.[9,21,22] A recent study reported on an AFM phase of V3Ga in the β-W structure.[23] The present magnetization measurements on bulk samples show a clear AFM behavior, in addition to a strong Meissner effect, indicating the presence of a superconducting transition temperature of 15 K.

Bulk samples of V_3Ga were synthesized via arc-melting using an Edmund Buehler MAM-1. The ingots were subsequently annealed at $1050\,^{\circ}C$ for 48 h in an argon environment to promote homogeneity and quenched in an ice bath. The composition was confirmed using energy dispersive spectroscopy (EDS) to be within $\pm2\%$ of the nominal composition. Magnetic measurements were performed on a Quantum Design MPMS XL-5 SQUID magnetometer with magnetic fields up to 5 T and at temperatures from $T = 2$ to 400 K. Synchrotron x-ray diffraction was measured at beamline 11-BM at the Advanced Photon Source (APS).[24] The structure was refined using TOPAS.[24] Overall, the structural analysis indicates the presence of both A15 and $D0_3$ phases of V_3Ga. Rietveld refinement in which the oxide contribution was not taken into account found 81% A15 and 19% $D0_3$ phases (see the supplementary material for further discussion.)

The results of magnetic measurements are shown in Figs. 2 and 3. In particular, Fig. 2 shows a magnetic hysteresis from the Meissner effect at low temperature, which is characteristic of flux pinning in the A15 type-II superconducting phase. The superconducting transition temperature $T_c = 13.6$ K is deduced from the plot of the magnetization as a function of temperature (Fig. 2, inset). This value of the critical temperature is in line with previous studies, although it is slightly lower than the maximal value reported for optimal stoichiometric V_3Ga.[25,26] It is likely that our A15 V_3Ga phase is slightly off-stoichiometry within the 2% error in our EDS measurements, thus giving rise to the slightly decreased critical temperature in our measurements. Magnetic susceptibility shown in the supplementary material indicates ~90% superconducting volume fraction, which is in line with the compositional analysis of the x-ray diffraction data through Rietveld refinement. The inset of Fig. 3 shows the magnetic moment as a function of applied field at $T = 300$ K. The moment is linear up to at least $\mu_0H = 5$ T, where the moment is only $\mu = 0.007\,\mu_B$ per formula unit (f.u.). This linear-in-H moment is similar to that we previously found in the AFM $D0_3$ phase of V_3Al.[9] The H_{c2} of our A15 phase is about 3.5 T for isothermal magnetization at 10 K (see the supplementary material), which is lower than the currently accepted value of 15 T at 10 K for A15 V_3Ga.[26,27] The decrease in H_{c2} is most likely due to the decreased T_c of
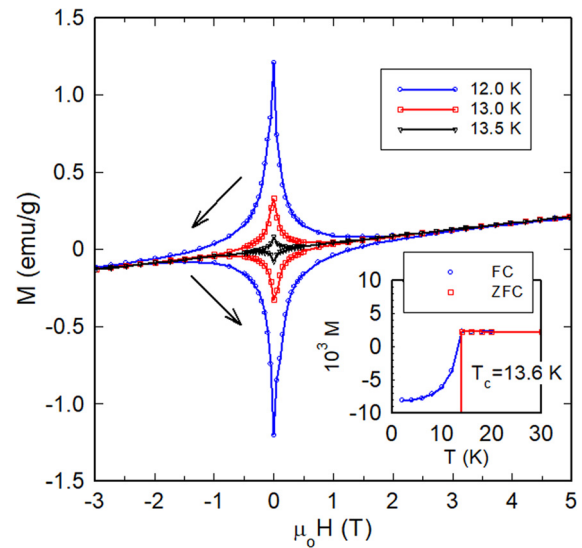

FIG. 2. Magnetization of V_3Ga vs magnetic field at low temperatures under zero field cooling (ZFC), showing a hysteretic peak around $\mu_0H = 0$ characteristic of flux pinning in a type-II superconductor. The inset shows the temperature-dependent Meissner flux exclusion below $T_C = 13.6$ K taken in a field of $\mu_0H = 0.05$ T.

the superconducting phase. The reduced T_c could result from the presence of the antiferromagnetic phase causing disorder in the compound, the possible off-stoichiometry, or grain size effects. Grain size effects on H_{c2} cannot be ruled out; however, since our synthesis method and those previously reported are similar, it is unlikely that grain size for the as-synthesized A15 V_3Ga phase would differ drastically from those previous reports.[26,27] Notably, off-stoichiometry of A15 V_3Ga[26] in previous studies was reduced T_c to a larger degree that what we observed;
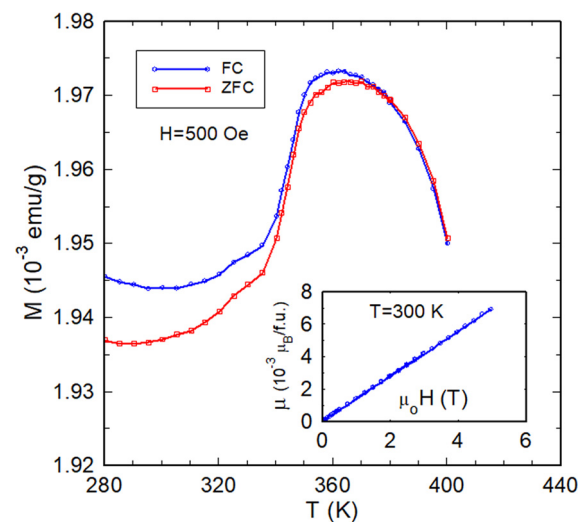

FIG. 3. Magnetic properties of AFM V_3Ga vs temperature and magnetic field. Magnetization vs temperature taken at $\mu_0H = 0.05$ T shows a peak at 360 K, indicating a magnetic transition. Inset: Magnetic moment vs magnetic field taken at $T = 300$ K, showing a small moment of only $\mu = 0.007\,\mu_B$/f.u. at $\mu_0H = 5$ T.

TABLE I. Calculated equilibrium properties of various magnetic states (Mag. st.) of V_3Ga. Lattice constants (a_0 in Å), atom-resolved and total magnetic moments (μ_{V_i} and μ_{tot} in μ_B/f.u.), total energy (E_0 in eV/atom), and the energy difference between the D0$_3$ and A15 structures (ΔE in meV/atom) are given. The results are based on various exchange-correlation approaches (LDA, GGA, GGA+U, and SCAN) as described in the text. For the A15 structure, the SCAN solutions for the FM and AFM-III states, which lie within 5 meV/atom, are nearly degenerate. See the supplementary material for details.

	D0$_3$ Mag. st.	a_0	μ_{V_1}	μ_{V_2}	μ_{V_3}	μ_{tot}	E_0	A15 Mag. st.	a_0	μ_{V_1}	μ_{V_2}	μ_{V_3}	μ_{tot}	E_0	ΔE
LDA	AFM	5.902	0.429	−0.429	0.0	0.0	−8.487	FM	4.678	0.089	0.164	0.112	0.368	−8.572	85
GGA	AFM	6.064	−1.314	1.314	0.0	0.0	−7.600	FM	4.788	0.222	0.390	0.303	0.916	−7.645	45
GGA+U	AFM	6.130	−1.916	1.917	0.0	0.0	−6.647	AFM-III	4.879	±1.351	±1.508	±1.502	0.0	−6.632	−15
SCAN	AFM	6.035	−1.848	1.848	0.0	0.0	−17.486	FM	4.744	0.308	0.523	0.414	1.245	−17.442	−44
								AFM-III	4.744	±0.268	±0.326	±0.330	0.0	−17.437	…

a reduction of 1.7 K was shown to be cause by the stoichometry being off by 10%, much larger than in our samples. It is reasonable to attribute some of the decrease in T_c to the AFM signal of another magnetic V_3Ga phase present in the as-synthesized compound mixture.

At higher temperatures, there is a notable peak in the temperature dependence of the low-field ($\mu_0H = 0.05$ T) moment at $T = 360$ K, shown in Fig. 3. A similar feature was seen in the temperature-dependent resistivity of V_3Ga at 350 K;[23] however, the peak was not assigned to a magnetic transition. Similar temperature-dependent features in both the magnetization and resistivity could arise from either a magnetic or a magnetostructural transition. A small peak in the magnetization of an antiferromagnet is generally characteristic of a Néel temperature,[9] so there is a reasonable case to assign the small peak observed here in the magnetization of V_3Ga to a magnetic transition.

In order to interpret our experimental results, first-principles electronic structure calculations were carried out within the framework of the DFT as implemented in the VASP software package.[28,29] Various approximations for the exchange-correlation energy employed to check the robustness of our results include the local-density approximation (LDA),[30] the generalized-gradient approximation (GGA),[31–33] GGA+U with Hubbard U correction, and the strongly constrained and appropriately normed (SCAN) meta-GGA.[34–36] Lattice and spin relaxations were included in the computations. Total energies and residual forces were converged to an accuracy of 10^{-8} eV and 10^{-7} eV/Å, respectively. Following He et al.,[23] $U = 2.0$ eV and $J = 0.67$ eV were used in GGA+U calculations.

The equilibrium properties of various magnetic states of V_3Ga are summarized in Table I (see the supplementary material for details). Electron correlation effects beyond the GGA as seen from the energy differences (ΔE) for the GGA+U and SCAN results tend to stabilize the D0$_3$ with respect to the A15 structure. Both LDA and GGA yield a ferromagnetic (FM) ground state for the A15 phase. With an improved treatment of electron correlations using the GGA+U and SCAN, however, the ground state becomes the AFM G-type D0$_3$ solution. Regarding the A15 solution, the effect of correlations is to stabilize the AFM-III state[23] (see the supplementary material) with respect to the FM solution. Within SCAN, the FM and AFM-III solutions in the A15 structure are almost degenerate and lie within 5 meV/atom (FM is marginally more stable). GGA+U, however, fully stabilizes the AFM-III solution. The AFM-III solution with a net zero magnetic moment is representative of the superconducting properties of the A15 structure.

Given the observation of the dual phase in the present V_3Ga samples, SCAN seems to exaggerate the stabilization of the D0$_3$ solution, while GGA+U gives almost degenerate A15 and D0$_3$ solutions within 15 meV/atom, which is in better accord with the experimental results and in agreement with previous DFT students.[23] We note that SCAN is known to exaggerate magnetic moments in some materials.[37–40]

Figure 4 compares the calculated electronic density of states (DOS) for the AFM D0$_3$ solution using various schemes. LDA and GGA essentially yield a gapless semiconductor, while the correlation effects beyond the GGA within GGA+U and SCAN lead to the opening of a bandgap of about 0.2 eV. Similar gap openings have been observed by Buchelnikov et al.[41] in other Heusler alloys.

We have estimated the magnetic transition temperature for the AFM G-type D0$_3$ phase based on our GGA solution. Using Monte Carlo simulations with ab initio exchange integrals and a Heisenberg model (see the supplementary material) we obtain the Néel temperature $T_N = 590$ K, which is higher than the peak position in the experimental $M(T)$ data at 360 K in Fig. 3. In order to account for disorder effects, we also calculated the Néel temperature using the mean field approximation within the SPR-KKR scheme (see the supplementary material for details). Figure 5 shows how T_N collapses rapidly with increasing disorder (x) when the Ga atoms are exchanged randomly with the nonmagnetic V atoms that lie between the two antiferromagnetically coupled magnetic V atoms. T_N is observed to go to zero at $x = 0.2$ or at the 20% exchange level. In particular, a reduction of the Néel temperature to $T_N = 360$ K would require only 6% of the Ga atoms exchanging with nonmagnetic V atoms. Note, however, that there is a sizeable energy barrier for V-Ga exchange. Nevertheless, the results of Fig. 5 emphasize the sensitivity of the Néel temperature to disorder effects.

In summary, we discuss the magnetism and superconductivity of V_3Ga. We show that this compound can crystallize in two distinct crystal structures: A15 that is superconducting and D0$_3$ that is an antiferromagnetic gapless semiconductor. At low temperatures, these two crystal structures are found to co-exist. Our experimental findings are supported by our in-depth first-principles computations using several different exchange-correlation functionals, which allow us to conclude that the ground states of A15 and D0$_3$ phases of V_3Ga are nearly degenerate. The Néel temperature of the ideal AFM D0$_3$ phase of V_3Ga is theoretically estimated to be 590 K, which is higher than the experimental peak at 360 K in the magnetization. We show, however, that the Néel temperature is quite sensitive to disorder effects
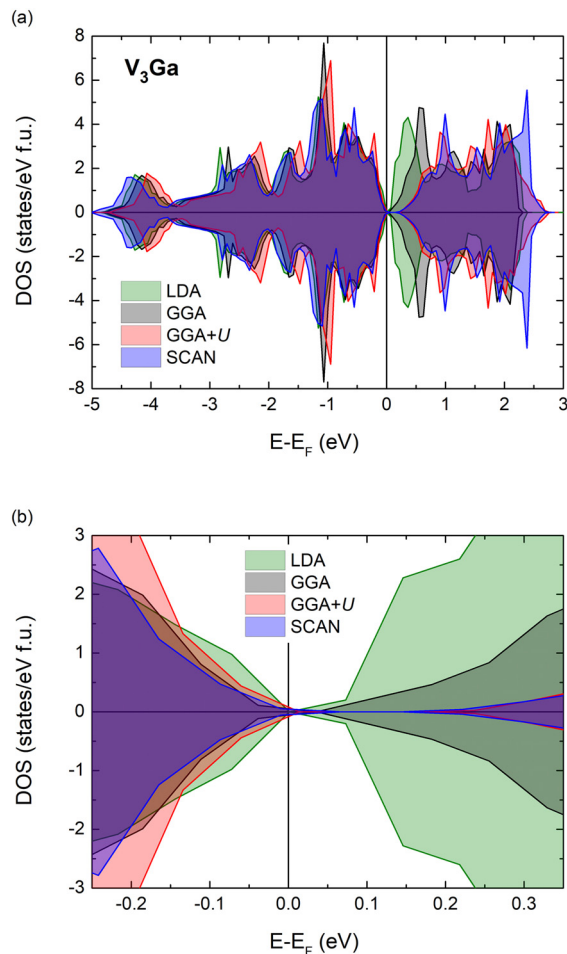
FIG. 4. (a) Comparison of the total DOS for the AFM D0$_3$ structure obtained using the LDA, GGA, GGA+U, and SCAN. (b) The gapless region near the Fermi level in (a) is shown on an expanded energy scale.
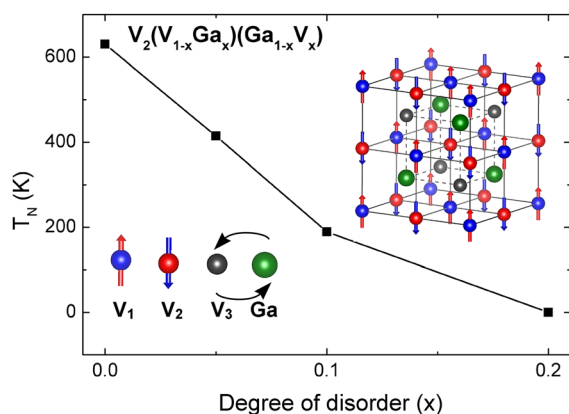

FIG. 5. Effect of disorder on the Néel temperature T_N of V$_3$Ga based on computations using the SPR-KKR scheme (see the supplementary material for details). x denotes the fraction of Ga atoms that are randomly exchanged with the nonmagnetic V atoms.

involving random exchange of Ga and non-magnetic V atoms and that the smaller experimental value of the Néel temperature could be achieved through as small as 6% Ga/V substitution. Our study demonstrates the dual-phase nature of V$_3$Ga and suggests that this material could provide a unique platform for exploiting co-existing superconducting and antiferromagnetic properties for quantum technology applications.

See the supplementary material for the additional data. The theoretical part includes details and subsequent results of VASP, SPR-KKR, and Monte Carlo calculations for ordered and disordered structures. The experimental part contains the discussion concerning the Rietveld analysis and superconductivity, and x-ray absorption spectroscopy measurements.

DATA AVAILABILITY

The data that support the findings of this study are available from the corresponding author upon reasonable request.

REFERENCES

[1]P. C. Canfield, P. L. Gammel, and D. J. Bishop, Phys. Today **51**(10), 40 (1998).
[2]P. A. Lee, N. Nagaosa, and X.-G. Wen, Rev. Mod. Phys. **78**, 17 (2006).
[3]Y. Mizuguchi and Y. Takano, J. Phys. Soc. Jpn. **79**, 102001 (2010).
[4]M. D. Lumsden and A. D. Christianson, J. Phys.: Condens. Matter **22**, 203203 (2010).
[5]Y. Du, G. Z. Xu, X. M. Zhang, Z. Y. Liu, S. Y. Yu, E. K. Liu, W. H. Wang, and G. H. Wu, Europhys. Lett. **103**, 37011 (2013).
[6]A. Bansil, S. Kaprzyk, P. Mijnarends, and J. Toboła, Phys. Rev. B **60**, 13396 (1999).
[7]L. R. Testardi, T. Wakiyama, and W. A. Royer, J. Appl. Phys. **48**, 2055 (1977).

[8]S. Ohshima, H. Ishida, T. Wakiyama, and K. Okuyama, Jpn. Soc. Appl. Phys. **28**, 1362 (1989).

[9]M. E. Jamer, B. A. Assaf, G. E. Sterbinsky, D. Arena, L. H. Lewis, A. A. Saúl, G. Radtke, and D. Heiman, Phys. Rev. B **91**, 094409 (2015).

[10]G. Gao and K. Yao, Appl. Phys. Lett. **103**, 232409 (2013).

[11]I. Galanakis, S. Tirpanci, K. Özdoğan, and E. Şaşioğlu, Phys. Rev. B **94**, 064401 (2016).

[12]L. Toikka, New J. Phys. **21**, 113033 (2019).

[13]W. Markiewicz, E. Mains, R. Vankeuren, R. Wilcox, C. Rosner, H. Inoue, C. Hayashi, and K. Tachikawa, IEEE Trans. Magn. **13**, 35 (1977).

[14]B. T. Matthias, E. A. Wood, E. Corenzwit, and V. B. Bala, J. Phys. Chem. Solids **1**, 188 (1956).

[15]M. Weger, Rev. Mod. Phys. **36**, 175 (1964).

[16]Y. A. Izyumov and Z. Kurmaev, Sov. Phys. Usp. **17**, 356 (1974).

[17]L. R. Testardi, Rev. Mod. Phys. **47**, 637 (1975).

[18]B. M. Klein, L. L. Boyer, D. A. Papaconstantopoulos, and L. F. Mattheiss, Phys. Rev. B **18**, 6411 (1978).

[19]T. Jarlborg and P. O. Nilsson, J. Phys. C **12**, 265 (1979).

[20]A. Jain, S. Ong, G. Hautier, W. Chen, W. Richards, S. Dacek, S. Cholia, D. Gunter, D. Skinnerand, G. Ceder, and K. Persson, APL Mater. **1**, 011002 (2013).

[21]M. E. Jamer, G. E. Sterbinsky, G. M. Stephen, M. C. DeCapua, G. Player, and D. Heiman, Appl. Phys. Lett. **109**, 182402 (2016).

[22]M. E. Jamer, Y. J. Wang, G. M. Stephen, I. J. McDonald, A. J. Grutter, G. E. Sterbinsky, D. A. Arena, J. A. Borchers, B. J. Kirby, L. H. Lewis, B. Barbiellini, A. Bansil, and D. Heiman, Phys. Rev. Appl. **7**, 064036 (2017).

[23]B. He, Z. Bao, K. Zhu, W. Feng, H. Sun, N. Pang, N. Tsogbadrakh, and D. Odkhuu, Phys. Status Solidi RRL **13**, 1900483 (2019).

[24]A. A. Coelho, J. Appl. Crystallogr. **51**, 210 (2018).

[25]S. Abe, T. Kadokura, T. Yamaguchi, T. Shinoda, and Y. Oya-Seimiya, J. Low Temp. Phys. **130**, 477 (2003).

[26]S. Foner, E. McNiff, Jr., S. Moehlecke, and A. Sweedler, Solid State Commun. **39**, 773 (1981).

[27]D. Decker and H. Laquer, J. Appl. Phys. **40**, 2817 (1969).

[28]G. Kresse and J. Furthmüller, Phys. Rev. B **54**, 11169 (1996).

[29]G. Kresse and D. Joubert, Phys. Rev. B **59**, 1758 (1999).

[30]J. P. Perdew and A. Zunger, Phys. Rev. B **23**, 5048 (1981).

[31]J. Perdew, Physica B **172**, 1 (1991).

[32]K. Burke, J. Perdew, and M. Ernzerhof, Int. J. Quantum Chem. **61**, 287 (1997).

[33]J. Perdew, K. Burke, and M. Ernzerhof, Phys. Rev. Lett. **77**, 3865 (1996).

[34]J. P. Perdew, S. Kurth, A. C. V. Zupan, and P. Blaha, Phys. Rev. Lett. **82**, 2544 (1999).

[35]J. Tao, J. P. Perdew, V. N. Staroverov, and G. E. Scuseria, Phys. Rev. Lett. **91**, 146401 (2003).

[36]J. Sun, A. Ruzsinszky, and J. P. Perdew, Phys. Rev. Lett. **115**, 036402 (2015).

[37]E. B. Isaacs and C. Wolverton, Phys. Rev. Mater. **2**, 063801 (2018).

[38]Y. Fu and D. J. Singh, Phys. Rev. Lett. **121**, 207201 (2018).

[39]M. Ekholm, D. Gambino, H. J. M. Jönsson, F. Tasnádi, B. Alling, and I. A. Abrikosov, Phys. Rev. B **98**, 094413 (2018).

[40]D. Mejia-Rodriguez and S. B. Trickey, Phys. Rev. B **98**, 115161 (2018).

[41]V. D. Buchelnikov, V. V. Sokolovskiy, O. N. Miroshkina, M. A. Zagrebin, J. Nokelainen, A. Pulkkinen, B. Barbiellini, and E. Lähderanta, Phys. Rev. B **99**, 014426 (2019).